POLITECNICO DI TORINO
Repository ISTITUZIONALE

Antibacterial and Antiviral Activities of Silver Nanocluster/Silica Composite Coatings Deposited onto Air Filters

Original
Antibacterial and Antiviral Activities of Silver Nanocluster/Silica Composite Coatings Deposited onto Air Filters / Luceri, A., Francese, R., Perero, S., Lembo, D., Ferraris, M., Balagna, C.. - In: ACS APPLIED MATERIALS & INTERFACES. - ISSN 1944-8244. - 16:3(2024), pp. 3955-3965. [10.1021/acsami.3c13843]

Availability:
This version is available at: 11583/2985081 since: 2024-01-15T15:55:23Z

Publisher:
American Chemical Society

Published
DOI:10.1021/acsami.3c13843

Terms of use:

This article is made available under terms and conditions as specified in the corresponding bibliographic description in the repository

Publisher copyright
ACS postprint/Author's Accepted Manuscript

This document is the Accepted Manuscript version of a Published Work that appeared in final form in ACS APPLIED MATERIALS & INTERFACES, copyright © American Chemical Society after peer review and technical editing by the publisher. To access the final edited and published work see http://dx.doi.org/10.1021/acsami.3c13843.

(Article begins on next page)

31 October 2026

This document is confidential and is proprietary to the American Chemical Society and its authors. Do not copy or disclose without written permission. If you have received this item in error, notify the sender and delete all copies.

Antibacterial and antiviral activities of silver nanocluster/silica composite coatings deposited onto air filters

Journal:	*ACS Applied Materials & Interfaces*
Manuscript ID	am-2023-13843k.R1
Manuscript Type:	Article
Date Submitted by the Author:	n/a
Complete List of Authors:	Luceri, Angelica; Politecnico di Torino, DISAT Francese, Rachele; Università degli Studi di Torino, Department of Clinical and Biological Sciences Perero, Sergio; Politecnico di Torino, Lembo, David; Universita degli Studi di Torino, Department of Clinical and Biological Sciences Ferraris, Monica; Politecnico di Torino, DISAT Balagna, Cristina; Politecnico di Torino

SCHOLARONE™
Manuscripts

Antibacterial and antiviral activities of silver nanocluster/silica composite coatings deposited onto air filters

Angelica Luceri[1], Rachele Francese[2], Sergio Perero[1], David Lembo[2], Monica Ferraris[1], Cristina Balagna[1,*]

[1]*Department of Applied Science and Technology, Politecnico di Torino, Corso Duca degli Abruzzi 24, 10129 Turin, Italy*

[2]*Department of Clinical and Biological Sciences, Laboratory of Molecular Virology and Antiviral Research, University of Turin, Regione Gonzole 10, 10043 Orbassano (TO), Italy;*

*Corresponding author:
Tel.: +39 011 0904325
Fax : +39 011 0904699
E-mail address: cristina.balagna@polito.it

Abstract

The indoor air quality should be better controlled and improved to avoid numerous health issues. Even if different devices are developed for air filtration, proliferation of microorganisms under certain conditions must be controlled. For this purpose, a silver nanoclusters/silica composite coating was deposited via co-sputtering technique, onto fiber-glass and polymeric based substrates. The aim of this work is focused on the evaluation of antibacterial and antiviral effect of the developed coating. The preliminary results of the compositional and morphological tests, showed an evenly distributed coating on filters surfaces. Several antibacterial tests were performed, confirming strong effect both in qualitative and quantitative methods, against *S. Epidermidis* and *E. Coli*. To understand if the coating can stop the proliferation of bacteria colonies spread on it, simulation of everyday usage of filters was performed, nebulizing bacteria solution with high colonies concentration and evaluating the inhibition of bacteria growth. Additionally, a deep understanding of the virucidal action and mechanism of Ag nanoclusters of the coating was performed. The effect of the coating both in aqueous medium and in dry methods was evaluated, in comparison with analysis on ions release. The virucidal performances are assessed against the *Human coronavirus OC43* strain (HCoV–OC43).

Keywords: Silver, composite coating, virucidal, antibacterial, filters, sputtering

1. Introduction

The poor quality of indoor air can have dire consequences on the health, comfort, and productivity of people inside buildings. In general, a decrease in the air quality level is caused by airborne pollutants, which are mainly constituted by bacteria, viruses, and fungi, (known as 'bioaerosols'), by non-organic particles, such as dust and tobacco smoke, as well as by certain occupants, such as pets, or even by the building materials and organic waste [1–3]. Therefore, air purification becomes of fundamental importance for indoor environments, but also considering that people spend about 90% of their time indoors [4–7].

Since such airborne particles may be very small and light, they can flow easily from one place to another [8]. When bioaerosol particles have a size within the 0.01-100 μm range, they can be inhaled, enter the respiratory tract and reach secondary organs, thereby causing numerous health problems, such as asthma, allergies, and several infectious diseases [2,9,10].

Air filtration technologies are able to improve indoor air quality by retaining airborne microorganisms and drastically reducing their amounts, but bacteria, fungi, and spores can proliferate in Heating, Ventilation and Air Conditioning (HVAC) systems, especially under certain temperatures, moisture, and dirt accumulation conditions. In addition, the growth of microorganisms on the surfaces of HVAC systems decreases the filtering performances and deteriorates the system, with a possible release of microorganisms in the indoor environment [11–13].

Therefore, a durable filtration device, capable of preventing the proliferation and spread of microorganisms, is needed to avoid these problems.

In the context of High Efficiency Particulate Air (HEPA) filters and HVAC systems, researchers have developed modification techniques for existing systems to create devices with dual functionalities, encompassing effective filtration and virucidal or antibacterial effects. Novel materials are also explored for this purpose. Notably, *Mallakpour et al.* [15] and *Madushani et al.* [16] extensively discussed various options for potential new air filter devices. Surface functionalization techniques, such as those involving tannic-acid [17] or hybrid materials [18] and the incorporation of antiviral and antibacterial agents, such as aluminum, zinc or copper oxide [19-21], contribute to the development of nanocoatings with antimicrobial effects [22-25]. These newly developed materials have been extensively tested on a broad spectrum of microorganisms, including bacteria, fungi, and viruses [17-21, 23-28], yielding generally satisfactory results. Moreover, many studies underscore the importance of environmentally friendly technique [26,27], aligning with a key objective of the present research.

In more detail, among the various proposed methodologies, particularly metallic nanoparticles such as gold, silver, and copper as antiviral/antibacterial agent are widely use, for their well- known antimicrobial effects [29-33]. Silver nanoparticles, or nanoclusters (AgNPs), have in particular shown an

antimicrobial effect towards a wide spectrum of bacteria and viruses, including *Staphylococcus Aureus, Escherichia Coli* [34,35]*, HIV* [36,37] *,* and the *Influenza A virus* [38,39]. AgNPs have recently also shown an antiviral effect towards coronaviruses, including the SARS-CoV-2 virus, which caused the Covid-19 pandemic in 2020. For this reason, AgNPs have been used to produce sprays and common mouthwash solutions[40], or in individual protective equipment, such as facial masks [41,42].

However, the mechanism behind the conference of antimicrobial properties to silver nanoparticles is not yet well known, but is probably the result of a combination of the reactive nature of AgNPs and the release of silver ions, which are able to form a bond with the bacterium cell wall, destroy its membrane, and inhibit cell replication [43].

To better understand the interaction between microorganisms and AgNPs, the influence of factors such as size, dimension, and concentration on the microbicidal effect is widely explored in literature. It is widely demonstrated that nanoparticles with dimensions less than 100 nm are commonly used in antimicrobial and antiviral applications, with the greatest efficacy observed in smaller particles due to the ratio between the exposed surface area and volume [44 45 46 47 48]. Moreover, smaller nanoparticles can readily interact with bacteria and viruses, penetrating the membrane and causing its destruction. Concentration also plays a pivotal role: as the nanoparticle quantity increases, the observed effect becomes stronger [49 50 51]. However, an excess of silver nanoparticles could lead to cytotoxic effects [52, 53]. During the nanoparticle synthesis, it is also feasible to control their shape. Although nanorods or nanowires can be obtained, spherical nanoparticles have been shown to exhibit superior with microorganisms, facilitating the inhibition of viral replication and proliferation[54, 55].

AgNPs can be synthesised via chemical, physical or biological methods [57]. *Haggag et al*. tried to synthesise silver nanoparticles through the green method, starting from air-dried powder of *L. coccineus* and *M. lutea,* in order to avoid the use of chemicals and the production of waste, and to obtain nanoparticles that could be used in biomedical applications to reduce cytotoxicity or pollution problems [58]. AgNPs obtained by means of a biological method are usually larger in size than those obtained through an electrochemical process [50].

In some instances, chemically synthesized AgNPs are incorporated into an organic or non-organic matrix, serving a dual purpose of preventing the dispersion of nanoparticles in the surrounding environment and ensuring a gradual and controlled release of silver. This results in a prolonged lifetime of the device [43,44]. AgNP/chitosan composites have indeed demonstrated antiviral effects against the H1N1 Influenza A virus [44]. The antiviral effect was exclusively attributed to the presence of silver, while the chitosan matrix proved instrumental in preventing the dispersion of nanoparticles into the environment.

Commercial silver nanoparticles have also been dispersed in a carbon foam matrix to prevent coalescence during synthesis. However, the bond between AgNPs and a carbon foam matrix was weak, leading to easy release of nanoparticles from the matrix. This resulted in close interaction with the HIV-1 virus, but also increased their toxicity [36]. Some systems incorporate silver nanoparticles for their antibacterial and virucidal effects within a silica matrix. The use of silica offers advantages, including preventing the agglomeration of nanoparticles. For instance *Acharya et al*. [59] conducted a study comparing the effects of Ag Nps and Ag-doped SiO_2 NPs against various bacteria. They found that the presence of a silica shell surrounding AgNPs enhanced their antibacterial activity by prolonging the release of Ag ions. Similar effects were observed using silica as a shell for AgCl nanoparticles, as demonstrated by *Tan et al.*[60]. Due to these benefits, systems composed of silver/silica nanoparticles have been employed in HVAC production to limit the proliferation of bacteria and to inactivate viruses. Various approaches can be used for the filter production, with a common method involving the creation of silver/silica nanoparticle systems for coating air filters. Air filter media coated with AgNPs or AgNPs-coated SiO_2 spheres, have shown a strong antiviral effect against bacteriophage MS2, without altering the filtration performances [61,62]. *Haeng et al*. [61] used AgNPs-coated nano-silica particles to coat air filters, providing effective virucidal action against MS2 viruses. To avoid the use of liquid in the coating process, studies on dry aerosol coatings have been conducted. *Park et al.* [23] developed a system for producing aerosolized SiO_2-Ag nanoparticles, which are dried using a sheath air flow, for coating air filters. This approach maintains filtration performance while imparting antiviral properties to the filters.

An alternative method involves incorporating the SiO_2-Ag system into a material, typically a polymeric matrix. This is exemplified by membranes obtained by *Wu et al.* [63], who electrospun PVDF/SiO_2 solution with silver nitrate as the precursor for AgNPs to produce PVDF/SiO_2/Ag composite nanofiber membranes. These membranes exhibit good mechanical and antibacterial properties, coupled with superhydrophobicity and self-cleaning capacity, making them suitable for HEPA applications. They also attempted to achieve a multilayer filter material by alternating layers of PVDF/SiO_2/Ag composite nanofiber with PET non-woven fabric. The high filtration efficiency of the membranes and strong antiviral capability make this system promising for the production of new filtration systems. To understand the role of silica in the antiviral effect within these systems, *Assis et al.*[64] immobilized silica/Ag particles within a polymeric matrix and tested the system against bacteria (*S. aureus* and *E. coli*) and the SARS-CoV-2 virus. They concluded that the antibacterial and antiviral effects of the system are due to the surface plasma resonance effect, enhanced by the simultaneous presence of Ag anchored to silica. This makes the SiO_2/Ag system potentially applicable in various devices requiring biocidal action, such as HVAC systems.

In this context, a silver nanocluster/silica composite coating, deposited by means of co-sputtering, has been developed by the authors [65–68]. The presence of a silica matrix allows the gradual release of silver ions, in a controlled manner, and prevents the dispersion of nanoclusters in the environment [69]. The coating has already been deposited and studied on several substrates for different applications, including aerospace structures [70,71], biomedical implants [72,73], and textiles [69], [71], [74]. Some studies about the antimicrobial and antiviral properties of the coating have also been performed using glass-fibre and metallic air filters as substrates [75,76].

The aim of this work has been to evaluate the antibacterial and antiviral activities of silver nanocluster/silica composite coatings deposited, via a co-sputtering technique, onto glass-fibre and polymeric air filters. To this aim, the antibacterial properties of the coated filters were analysed against two bacterial strains, that is, *Staphylococcus epidermidis* and *Escherichia coli,* and their virucidal activity was verified against a *Beta-coronavirus* through tests in an aqueous medium/screening assay, using a drying method, and by means of an ion release test. The antiviral mechanism of these composite coatings is discussed hereafter.

2. Materials and Methods

2.1 Coating deposition

The coatings are composed of silver nanoclusters embedded in a silica matrix and deposited, by means of a patented co-sputtering process [39], onto glass-fibre and polymeric air filters, named *Glass* and *Pol* in the text, respectively, provided by GV Filtri Srl, Italy. The sputtering equipment was set up for two targets for each deposition, a silica one (Sigma-Aldrich™ 99.99% purity) and a silver one (Franco Corradi S.r.l. 99.9% purity). A 200 W power was applied, in radio frequency mode (RF), to the silica target for both of the air filters, while different powers were applied to the silver target: 3 and 5 W, applied in direct current mode (DC), to the glass fibre-based filter (called *Glass-Ag3* and *Glass-Ag5* in the text), while 3 W was applied, in DC, to the polymeric filter (called *Pol-Ag3* in the text). All the depositions were performed for 1 hour in a pure argon atmosphere, under a pressure of 5.5 dPa.

2.2 Coating Characterization

Compositional analyses were conducted, by means of Energy Dispersive Spectroscopy (EDS, EDAX PV 9900TM), which allowed the atomic percentage of the elements constituting the coatings to be determined, that is, Si for the silica matrix and Ag for the silver nanoclusters.

Morphological analyses were performed, using a Field Emission Scanning Electron Microscope (FESEM, QUANTA INSPECT 200, Zeiss SUPRA™ 40™), at different magnifications, in order to verify that the deposition had occurred successfully with a homogeneous distribution of the silver nanoclusters inside the silica matrix. For this analysis, the in-lens detector was used with secondary electrons.

2.3 Leaching test in water

The amount of silver ions released by coated air filters was evaluated by means of a leaching test in milliQ water at room temperature. Samples (1x1 cm^2) were immersed in 30 ml of water, with the coated surface face up. The solutions were analysed after 3 hours, as well as after 1, 3, 7 and 14 days, by means of a spectrophotometer (Hanna Instruments™), and the concentration of silver ions was determined in ppm. Each measurement was performed in triplicate.

2.4 Antibacterial tests

The antibacterial properties of the coated air filters were evaluated by means of three different tests: inhibition halo test, dilution test and a bacterial contamination test.

2.4.1 Inhibition halo test

The inhibition halo test was performed according to the NCCLS M2-A9 Performance standard [77], and two non-pathogen bacteria, *Staphylococcus Epidermidis* (Gram +, ATCC14990) and *Escherichia Coli* (Gram -, ATCC8739) were tested. The bacterial solutions (McFarland index 0.5) were spread on Mueller Hinton agar plates. Coated and uncoated air filters (1x1 cm^2) were then placed onto the agar plates and incubated at 35°C for 24 h. After the incubation, the formation of a halo was observed around the samples and evaluated.

2.4.2 Dilution test

The dilution test was used to evaluate the number of colony-forming units (CFU) of *S. epidermidis* that had adhered to the surface samples and proliferated in the broth [78]. The starting solution for this test was a broth containing a standard number of bacteria, that is, of approximately 5 x 10^5 CFU/ml. Three uncoated and three coated air filters (2 x 0.5 cm^2) were immersed in the bacterial broth and incubated at 35°C for 24h. After incubation, the turbidity of each tube was evaluated and the dilutions were prepared with physiological solutions. In order to calculate the number of CFU that had adhered to the surface, the samples were removed from the broth, immersed in 3 ml of physiological solution water and vortexed for 5 minutes. These solutions were then diluted with other physiological solutions. Finally, an aliquot of the diluted solutions was spread onto a blood agar plate and incubated at 35°C for 24h. At this point, it was possible to count the number of CFU on each plate.

2.4.3 Contamination test

This test consists in the contamination of the filters in a control manner through a bacterial bioaerosol in order to simulate the HVAC system. This is an experimental set-up developed by author and already described in a previous paper[75]. The device is composed of a compressed air system, a bioaerosol generator (TOPAS ATM 220) and a filter holder. The bacterial aerosol was generated from a bacterial suspension containing a high concentration of *S. epidermidis* colonies (McFarland index 5.0) at an airflow of 3 bar. Bioaerosol was nebulized on the filter, put inside the filter holder, for 30 minutes. After the contamination, the filters were placed on Mueller Hinton plates and incubated at 35°C for 24 hours. Then, bacterial growth was evaluated around and below the filter surface. Three coated and one uncoated filter as control (diameter 4 cm) were tested.

2.5 Antiviral tests

The glass fibre and polymeric filters were subjected to different antiviral tests in order to evaluate the virucidal effect of the coating. The tests were performed by comparing coated and uncoated substrates.

2.5.1 Cell lines and viruses

Human lung MRC-5 fibroblast cells (ATCC® CCL-171) were propagated in Dulbecco's Modified Eagle Medium (DMEM; Sigma, St. Louis, MO, USA) supplemented with a 1% (v/v) penicillin/streptomycin solution (Euroclone, Milan, Italy) and heat inactivated with 10% (v/v) of foetal bovine serum (FBS, Sigma). The human coronavirus OC43 strain (HCoV–OC43) (ATCC® VR-1558) was propagated in MRC-5 cells at 33 °C, in a humidified 5% CO_2 incubator, and titrated in a focus-reduction assay in MRC-5 cells. After 20 h of incubation at 33 °C, the cells were fixed with cold acetone-methanol (50:50) and subjected to indirect immunostaining, using an anti-coronavirus monoclonal antibody (MAB9013, Merck, Darmstadt, Germany) and a peroxidase-conjugated AffiniPure F(ab')2 Fragment Goat Anti-Mouse IgG secondary antibody (H + L) (MAB9013, Jackson ImmunoResearch Laboratories Inc., West Grove, PA, USA). The number of immunostained foci was counted and the titer was expressed in terms of focus forming units per ml (FFU/ml). HCoV-OC43 has an extremely high structural homology with SARS-CoV-2, from both the phylogenetic and molecular points of view, and it has been used in several viral persistence/inactivation studies as a model substitute for the highly pathogenic SARS-1, SARS-2 and MERS coronaviruses [79,80].

2.5.2 Virucidal test in an aqueous medium/screening assay

This assay was performed as a first screening to evaluate any antiviral activity mediated by both a direct interaction of the virus with the silver nanocluster/silica composite coating deposited on the substrates and by the Ag ions released from the silver nanoclusters dispersed in the silica matrix of the coating. The experiment was performed as previously reported [76]. Briefly, an aliquot of

approximately 10^6 HCoV-OC43 of viral particles was resuspended in a final 500µl volume of a cell culture medium (DMEM), supplemented with 2% of serum. The virus + medium mixture was then incubated under continuous oscillation together with the samples (cut into1cm^2, coated or uncoated pieces) for 1h 30 min at room temperature. The same number of viral particles were incubated under the same experimental conditions, but without any samples, and used as a control. Subsequently, the pre-incubated virus + medium mixture was collected, and the residual viral infectivity was assessed, by means of titration on MRC-5 cells, as described above. Viral inactivation was determined by comparing the titer of the virus inoculated on the coated filters with that of the viral suspension inoculated on the uncoated filters. The Logarithm of inactivation (R) was calculated as follows: Log (Untreated sample) – Log (Treated sample).

2.5.3 Virucidal test through the drying method

This assay was designed to obtain preliminary results on the mechanism of action of the silver nanocluster/silica composite coatings. It was performed to evaluate whether the direct interaction of viral particles with the coatings could have been the cause of the titer reduction observed in the screening assay. A fixed virus inoculum (25µl, ~10^6 FFU) was inoculated onto samples cut into 1 cm^2 coated and uncoated pieces. In parallel, the same viral inoculum was placed into a sterile plastic support. The samples were then incubated at room temperature for 60 minutes until the 25µl initially inoculated onto the filters had completely dried. After the incubation, the samples were transferred to a sterile 24-well plate; an aliquot of 300µl of DMEM, supplemented with 20% FBS, was dispensed in each well and the plate was incubated at 150 rpm at room temperature for 15 minutes. Subsequently, three sequential 3sec vortexing passages were performed for each sample. These steps were necessary to recover the residual viral particles from the filters. Virus inactivation of the coating was evaluated by means of titration on MRC-5 cells, as described above. Inactivation was determined by comparing the titer of the inoculated virus on the coated filters with the titer of the inoculated suspension on the uncoated ones. The Logarithm of inactivation (R) was calculated as described above.

2.5.4 Ion release antiviral test

This assay was carried out to evaluate any indirect virucidal action mediated by the Ag + ions released by the nanostructured coatings. An aliquot of 500µl of DMEM+2%FBS was pre-incubated with the 1cm^2, coated and uncoated samples for 1h30 min at room temperature under continuous stirring. Subsequently, the pre-incubated medium containing any eventual Ag ions released from the coatings (ionic extract) was inoculated with 10^6 viral particles of HCoV-OC43. The viral particles were then incubated with the ionic extract under continuous oscillation for 1h30 min to ensure that the time condition was the same as that used for the virucidal assay conducted in an aqueous medium. At the

end of the treatment, the viral inactivation of the ionic extract was evaluated by means of titration on MRC5 cells, as described above. Virus inactivation was determined by comparing the titer of the virus incubated with the ion extract with the titer of the virus incubated with the control extract (the medium incubated with uncoated samples). The Logarithm of inactivation (R) was calculated as described above. To exclude the possibility of the uncoated filter releasing antiviral substances, an additional control was added to the assay: an aliquot of 500µl of DMEM+2%FBS was treated under the same time and temperature conditions, but without any sample.

2.5.5 Statistical analysis

The results were presented as the mean values of three independent experiments (mean ± SEM). One-way ANOVA and the Bonferroni test were used to assess the statistical significance of the differences between the treated and untreated samples, where appropriate (significance was set at $P < 0.05$).

3. Results and discussion

3.1 Compositional and morphological characterisation

Coating deposition occurred successfully on both the glass-fibre and polymeric air filters, as confirmed by the EDS analysis results reported in Table 1. Si, which was already present in the uncoated glass-fibre filter, was found to have increased, due to the deposited silica matrix. Ag was only detected on the coated substrates and increased from 0.9 to 1.6 at. % as the power applied to the target was increased. The polymeric filter only contained carbon, oxygen, and nitrogen before the coating deposition. Si and Ag appeared on the Pol-Ag3 sample with atomic percentages of about 1 and 0.8, respectively.

Fig. 1 reports FESEM images relative to the uncoated filters and silver nanocluster/silica composite coating deposited on the filters. The morphology of the analysed surfaces changed after deposition of the coating. The uncoated Glass filter (a) had a rather smooth surface, albeit with some scratches. The coated Glass-Ag5 filter (b) had a globular and porous surface, due to the silica matrix, with well-dispersed silver nanoclusters that were visible as bright nanosized particles (less than 50 nm). This morphology had already been observed in previous experiments [75,76] on glass-fiber-based filters subjected to the same coating deposition, but using another type of sputtering equipment.

The uncoated polymeric filter Pol (c) had a typical honeycomb structure, while the coating deposited on the Pol-Ag3 filter (d) showed a similar morphology to that observed on the Glass-Ag5 filter.

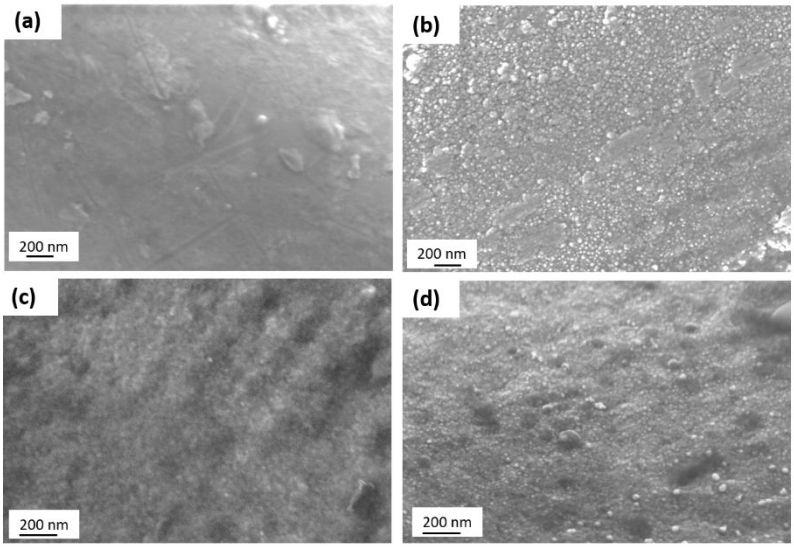


Fig.1: FESEM of the glass-fibre filters (a) Glass and (b) Glass-Ag5; polymeric filter (c) Pol and (d) Pol-Ag3

3.2 Release test in water

The precise mechanism of interaction between silver and bacteria or viruses is not fully known. However, both nanoparticles and ions play crucial synergistic roles in the interaction with microorganisms. It is well-known that silver ions are released into the surrounding environment from silver nanoparticles, as a function of their dimension, concentration, and of the covering agents that could coat the nanoparticles [81,82]. The silica matrix coating embeds silver nanoclusters and prevents their dispersion in the environment [69]: this feature is of fundamental importance because it prevents the occurrence of potential respiratory issues resulting from the inhalation of silver nanoparticles. In addition, the porous nature of the sputtered silica matrix also allows silver ions to be released from the embedded nanoclusters.

For this reason, the overall amount of silver ions released into water at room temperature was investigated: this test condition is far more severe than the environmental conditions in which air filters work, but it is useful to understand the kinetics of released silver ions as a function of time.

Figure 2 reports the release of the silver ions from the silver nanocluster/silica composite coated glass-fibre and polymeric filters. The quantity of ions detected in the water for the coated glass-fibre filters is about 0.2 ppm and 0.4 ppm for Glass-Ag3 and Glass-Ag5, respectively. Indeed, the higher the amount of silver in the coating is, the higher the leached amount. However, the value is about 0.5 ppm for the Pol-Ag3 filter, even though the Ag amount is similar to that of Glass-Ag3. The polymeric filter is probably easily soaked with water, and thus releases ions faster.

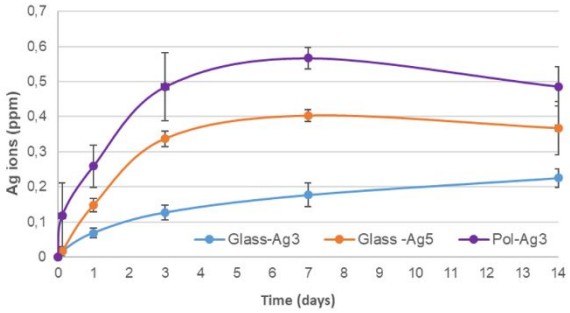


Fig.2: Test on the release of silver ions into water at room temperature from a silver nanocluster/silica composite coating on glass-fibre and polymeric air filters.

3.3 Antibacterial tests

Figure 3 shows the inhibition halo results of the silver nanocluster/silica composite coating deposited on both the (a) glass fibre and (b) polymeric filters against S. *epidermidis* and *E. coli*. A bacteria-free zone of about 3-5 mm is clearly visible around all the coated glass fibre and polymeric filters.

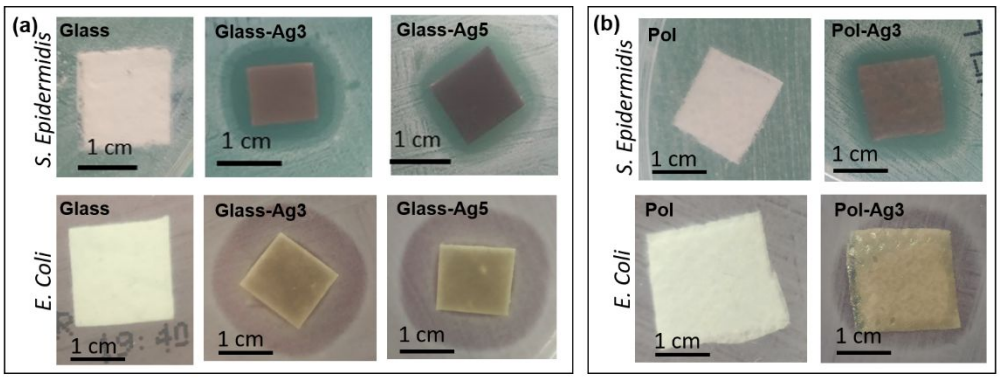


Fig.3: Inhibition halo test results against *S. epidermidis* and *E. coli*: (a) uncoated and coated glass fibre filters; (b) uncoated and coated polymeric filters.

No significant differences are evident when comparing the coating with higher silver content is to the one with less silver amount (Ag5 vs Ag3). However, it is noteworthy that the inhibition zone of Glass-Ag3 appears slightly larger compared to that obtained for Glass-Ag5. It is crucial to emphasize that this test is qualitative rather than quantitative. Furthermore, while the amount of Ag in Glass-Ag5 is higher than that in Glass-Ag3, the distribution of nanoclusters on the sample surface and within the matrix could vary. The inhibition halo did not form around the uncoated substrates, which means that bacteria were able to proliferate.

Since the inhibition halo evaluation is a qualitative test, a further antibacterial test of the CFU count was carried out in order to quantitatively assess the proliferation of bacteria and the adhesion of *S. epidermidis* onto samples. Figure 4 reports the histograms relative to the results of the CFU (a) proliferated in broth, and (b) the CFU that remained adhered to the sample surface and detected in the vortex solution.

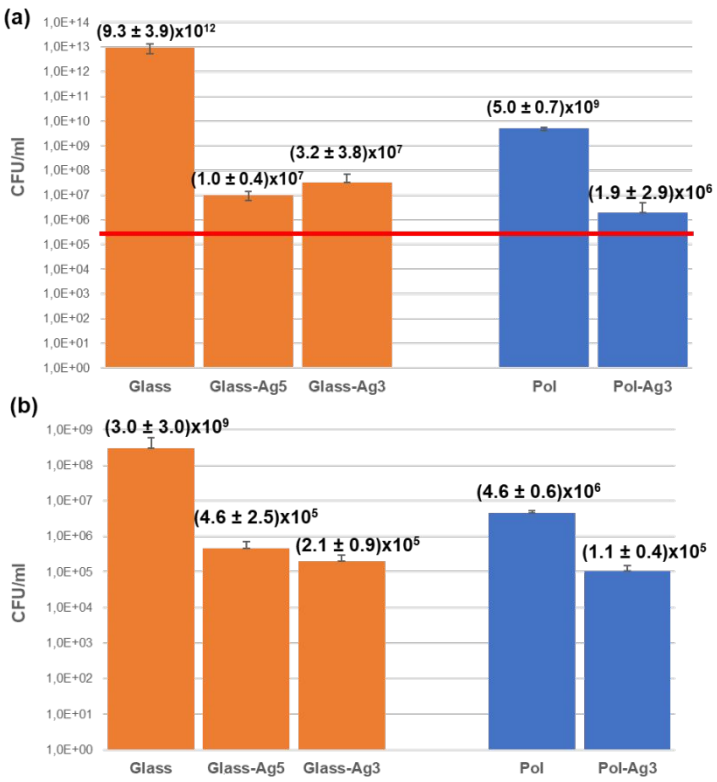


Fig.4: CFU count against *S. epidermis* of both the uncoated and coated glass-fibre and polymeric air filters: (a) broth solution used to evaluate bacteria proliferation; (b) vortex solution used to evaluate the adhesion of bacteria onto the sample surfaces.

As reported in the histograms in Fig. 4 (a), the silver nanocluster/silica composite coating reduced the bacterial proliferation in the broth by 3 and 5 orders of magnitude for the polymeric and glass fibre filters, respectively, even though only one side of the substrate had been coated. The vortex solution (Fig.4 b) registered a reduction of the CFU that had adhered to the coated sample surfaces. This decrement in number of CFU is more remarkable (of 4 orders of magnitude) for the glass fibre filters than that obtained for the polymeric filter (only one order of magnitude). No relevant difference was noted between the two samples with higher and lower amounts of silver, that is, Glass-Ag3 and Glass-Ag5.

The bacterial contamination test enabled the simulation of the filter performance in a HVAC system under operative conditions. This test was performed under rigorous conditions compared to the real-world scenario as the bacterial concentration within the bioaerosol was elevated. To achieve this, contamination is restricted to a 30-minute duration. Fig. 5 reports the photographs relative to the contaminated filters on the agar after the incubation. The coatings deposited on both Glass (Fig. 5 (a)) and Pol (Fig. 5 (b)) filters completely suppressed the proliferation of *S. epidermidis* colonies. Conversely, colonies grew on both uncoated filters. This experiment clearly demonstrates that the silver coating effectively exhibits bactericidal properties, preventing bacterial growth entirely.

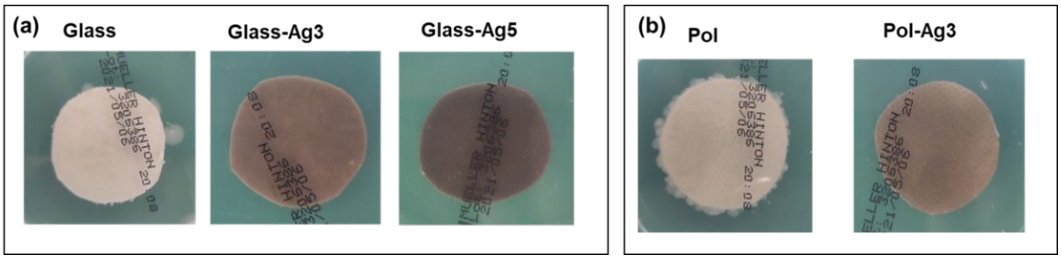


Fig. 5: Contamination test with *S. epidermidis* through bioaerosol generator on (a) uncoated and coated glass-fibre filter and (b) uncoated and coated polymeric membrane

3.4 Antiviral test

The first set of antiviral experiments was performed to evaluate the antiviral activity of the coatings when deposited on glass-fibre and polymeric filters. The antiviral experiments were performed according to previously published articles [28, 50]. The authors evaluated the antiviral efficacy of similar composite coatings, deposited on glass fibre filters, albeit with another type of sputtering equipment, against other respiratory viruses, such as the influenza virus, respiratory syncytial virus and rhinovirus [76]. In addition, the composite coating was deposited onto a disposable mask, and it was able to reduce the SARS-CoV-2 titre to zero [42]. The results of the virucidal test in an aqueous medium are summarised in Figure 6 and Table 2.

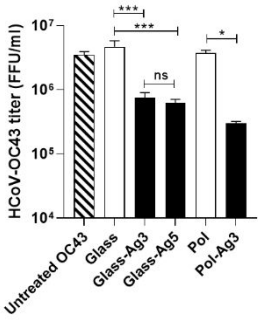


Fig. 6: Virucidal assay in an aqueous medium. Comparison of the coated and the uncoated samples. " Untreated" refers to the viral particles incubated under the same temperature and time conditions, but without testing any samples. The viral titre is reported on the Y-axis and expressed as focus forming units per ml (FFU/ml). The type of sample is reported on the X-axis. ***pANOVA<0.001;*pANOVA<0.05; ns: not significant.

Both the Glass-Ag3 and Glass-Ag5 samples demonstrate a significant reduction in the number of infectious HCoV-OC43 particles, compared to the uncoated glass fibre filter (Glass), of around 0.8 Log (logarithm of inactivation). No statistically significant difference was observed for the anti-CoV efficacy between the two coatings. Nevertheless, the Glass-Ag5 sample showed a numerically superior anti-CoV efficacy than Glass-Ag3, and it was therefore selected for the continuation of the study. The Pol-Ag3 sample also showed a significant anti-CoV activity, whereby the HCoV-OC43

titer was reduced by 1.1 Log, compared to the uncoated polymeric filter. Altogether, these results demonstrate that the analysed composite coatings are endowed with anti-OC43 properties regardless of the substrate on which they are deposited.

Two different antiviral tests were performed to preliminarily investigate the mechanism of action of the coatings when deposited on glass-fibre (Glass-Ag5) and polymeric (Pol-Ag3) air filters (Fig. 7).

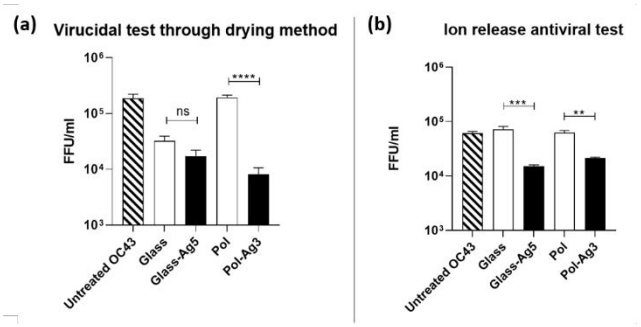


Fig. 7: Virucidal assay conducted by means of a drying method (a) and Ion release antiviral test (b). The coated and the uncoated samples are compared. "Untreated" refers to the viral particles incubated under the same temperature and time experimental conditions, but without testing any samples. The viral titre is reported on the Y-axis and expressed as focus forming units per ml (FFU/ml). The sample type is reported on the X-axis. ****pANOVA<0.0001 ***pANOVA<0.001; **pANOVA<0.01; ns: not significant.

The virucidal test, conducted through a drying method, was designed to evaluate whether the direct interaction of viral particles with the coating could be the cause of the virucidal activity observed in the previously described screening assay. Two different mechanisms were observed as a function of the air filter material, and numerical results are shown in Table3. In fact, the Pol-Ag3 samples (Fig. 7a) showed an anti-CoV efficacy that was comparable with that obtained in the screening assay. This suggests that the coating is able to directly alter and inactivate the viral particles, regardless of the ion release. In this case, the inactivation logarithm was about 1.4. On the other hand, the antiviral activity of Glass-Ag5 in an aqueous medium was mediated by the silver ions released from the coating (inactivation logarithm only 0.3) and the coated glass-fibre filter therefore did not show any direct virucidal activity.

The second antiviral test (Fig. 7b) was thus conducted to evaluate an indirect virucidal action mediated by the released silver ions. The Glass-Ag5 sample reduced the viral titer by about 0.7 Log, thus confirming that the virucidal action of the sample was mediated by the release of silver ions from the silver nanocluster/silica composite coating. The Pol-Ag3 filter also showed a residual anti-CoV action mediated by the ion extract (0.5 Log), and the mechanism of action was thus ascribable more to direct contact, thus verifying with the previous experiment.

This different behavior could be due to the different nature of the substrates: the polymeric filters had a larger porosity (up to 100 μm) than that of the glass-fiber filters (less than 20 μm). The coating was

also deposited on more internal fibers of the polymeric substrate and the infected cells were able to reach and adhere to them and interact more effective with the silver nanoclusters.

4. Conclusions

The composite coating made of silver nanoclusters that were embedded well within a silica matrix were successfully deposited onto glass-fibre and polymeric air filters by means of a co-sputtering technique. Morphological and compositional analyses confirmed the homogeneity of the coating on each substrate. Silver ion release tests were conducted in water for 14 days and they showed a gradual release of ions, which is known to be necessary to obtain a prolonged and continuous antibacterial effect of the coating. The coating showed antibacterial properties against Gram + and Gram – bacteria strains, that is, *S. epidermidis* and *E. coli*. A test of the inhibition halo, and a CFU count confirmed the strong antibacterial effect of the silver nanocluster/silica composite coating on both air filters. The antiviral activity of the composite coating was assessed against the human coronavirus OC43 strain. The virucidal mechanism of action of the coating seemed to be different on each substrate. The coated glass-fibre air filter demonstrated an indirect virucidal effect related to the release of silver ions, whereas the coated polymeric filter was able to directly alter and inactivate the viral particles. A direct virucidal action, demonstrated by means of the drying assay, could be more interesting for the application of coatings on materials in contact with air. On the other hand, the ion release-mediated mechanism of action means the coating would function better in an aqueous medium.

Acknowledgments

The authors would like to thank GV Filtri for supplying the air filters used as substrates in this research work.

This research was partially supported by EU funding within the MUR PNRR Extended Partnership initiative on Emerging Infectious Diseases (Project no. PE00000007, INF-ACT) to DL.

Data Availability Statement

Authors did not generate or use any data to prepare this paper.

Reference

(1) Kalogerakis, N.; Paschali, D.; Lekaditis, V.; Pantidou, A.; Eleftheriadis, K.; Lazaridis, M. Indoor Air Quality—Bioaerosol Measurements in Domestic and Office Premises. *J. Aerosol Sci.* **2005**, *36* (5–6), 751–761.

(2) Douwes, J.; Thorne, P.; Pearce, N.; Heederik, D. Bioaerosol Health Effects and Exposure Assessment: Progress and Prospects. *Ann. Occup. Hyg.* **2003**, *47* (3), 187–200.

(3) Nazaroff, W. W. Teaching Indoor Environmental Quality. *Indoor Air* **2016**, *26* (4), 515–516. https://doi.org/10.1111/ina.12309.

(4) Klepeis, N. E.; Nelson, W. C.; Ott, W. R.; Robinson, J. P.; Tsang, A. M.; Switzer, P.; Behar, J. V.; Hern, S. C.; Engelmann, W. H. The National Human Activity Pattern Survey (NHAPS): A Resource for Assessing Exposure to Environmental Pollutants. *J. Expo. Sci. Environ. Epidemiol.* **2001**, *11* (3), 231–252.

(5) Elder, A.; Gelein, R.; Silva, V.; Feikert, T.; Opanashuk, L.; Carter, J.; Potter, R.; Maynard, A.; Ito, Y.; Finkelstein, J. Translocation of Inhaled Ultrafine Manganese Oxide Particles to the Central Nervous System. *Environ. Health Perspect.* **2006**, *114* (8), 1172–1178.

(6) Oberdörster, G.; Utell, M. J. Ultrafine Particles in the Urban Air: To the Respiratory Tract--and Beyond? *Environ. Health Perspect.* **2002**, *110* (8), A440–A441.

(7) Semmler, M.; Seitz, J.; Erbe, F.; Mayer, P.; Heyder, J.; Oberdörster, G.; Kreyling, W. G. Long-Term Clearance Kinetics of Inhaled Ultrafine Insoluble Iridium Particles from the Rat Lung, Including Transient Translocation into Secondary Organs. *Inhal. Toxicol.* **2004**, *16* (6–7), 453–459.

(8) Van Leuken, J. P. G.; Swart, A. N.; Havelaar, A. H.; Van Pul, A.; Van der Hoek, W.; Heederik, D. Atmospheric Dispersion Modelling of Bioaerosols That Are Pathogenic to Humans and Livestock–A Review to Inform Risk Assessment Studies. *Microb. Risk Anal.* **2016**, *1*, 19–39.

(9) Górny, R. L.; Dutkiewicz, J. Bacterial and Fungal Aerosols in Indoor Environment in Central and Eastern European Countries. *Ann Agric Env. Med* **2002**, *9*, 17–23.

(10) Reponen, T.; Grinshpun, S. A.; Conwell, K. L.; Wiest, J.; Anderson, M. Aerodynamic versus Physical Size of Spores: Measurement and Implication for Respiratory Deposition. *Grana* **2001**, *40* (3), 119–125.

(11) Perrier, J. C. B.; Le Coq, L.; Andres, Y.; Le Cloirec, P. SFGP 2007-Microbial Growth onto Filter Media Used in Air Treatment Devices. *Int. J. Chem. React. Eng.* **2008**, *6* (1).

(12) Stolwijk, J. A. Sick-Building Syndrome. *Environ. Health Perspect.* **1991**, *95*, 99–100. https://doi.org/10.1289/ehp.919599.

(13) Ahearn, D. G.; Crow, S. A.; Simmons, R. B.; Price, D. L.; Mishra, S. K.; Pierson, D. L. Fungal Colonization of Air Filters and Insulation in a Multi-Story Office Building: Production of Volatile Organics. *Curr. Microbiol.* **1997**, *35* (5), 305–308.

(14) Bolashikov, Z. D.; Melikov, A. K. Methods for Air Cleaning and Protection of Building Occupants from Airborne Pathogens. *Build. Environ.* **2009**, *44* (7), 1378–1385.

(15) Mallakpour, S.; Azadi, E.; Hussain, C. M. Fabrication of Air Filters with Advanced Filtration Performance for Removal of Viral Aerosols and Control the Spread of COVID-19. *Adv. Colloid Interface Sci.* **2022**, *303*, 102653. https://doi.org/10.1016/j.cis.2022.102653.

(16) Dahanayake, M. H.; Athukorala, S. S.; Jayasundera, A. C. A. Recent Breakthroughs in Nanostructured Antiviral Coating and Filtration Materials: A Brief Review. *RSC Adv.* **2022**, *12* (26), 16369–16385. https://doi.org/10.1039/D2RA01567F.

(17) Kim, S.; Chung, J.; Lee, S. H.; Yoon, J. H.; Kweon, D.-H.; Chung, W.-J. Tannic Acid-Functionalized HEPA Filter Materials for Influenza Virus Capture. *Sci. Rep.* **2021**, *11* (1), 979. https://doi.org/10.1038/s41598-020-78929-4.

(18) Kasbe, P. S.; Gade, H.; Liu, S.; Chase, G. G.; Xu, W. Ultrathin Polydopamine-Graphene Oxide Hybrid Coatings on Polymer Filters with Improved Filtration Performance and Functionalities. *ACS Appl. Bio Mater.* **2021**, *4* (6), 5180–5188. https://doi.org/10.1021/acsabm.1c00367.

(19) Choi, D. Y.; Heo, K. J.; Kang, J.; An, E. J.; Jung, S.-H.; Lee, B. U.; Lee, H. M.; Jung, J. H. Washable Antimicrobial Polyester/Aluminum Air Filter with a High Capture Efficiency and Low Pressure Drop. *J. Hazard. Mater.* **2018**, *351*, 29–37. https://doi.org/10.1016/j.jhazmat.2018.02.043.

(20) Kim, J.-H.; Lee, G.-H.; Ma, J.; Lee, S.; Su Kim, C. Facile Nanostructured Zinc Oxide Coating Technique for Antibacterial and Antifouling Air Filters with Low Pressure Drop. *J. Colloid Interface Sci.* **2022**, *612*, 496–503. https://doi.org/10.1016/j.jcis.2021.12.139.

(21) Perelshtein, I.; Levi, I.; Perkas, N.; Pollak, A.; Gedanken, A. CuO-Coated Antibacterial and Antiviral Car Air-Conditioning Filters. *ACS Appl. Mater. Interfaces* **2022**, *14* (21), 24850–24855. https://doi.org/10.1021/acsami.2c06433.
(22) Choi, D.; Choi, M.; Jeong, H.; Heo, J.; Kim, T.; Park, S.; Jin, Y.; Lee, S.; Hong, J. Co-Existing "Spear-and-Shield" Air Filter: Anchoring Proteinaceous Pathogen and Self-Sterilized Nanocoating for Combating Viral Pandemic. *Chem. Eng. J.* **2021**, *426*, 130763. https://doi.org/10.1016/j.cej.2021.130763.
(23) Park, D. H.; Joe, Y. H.; Hwang, J. Dry Aerosol Coating of Anti-Viral Particles on Commercial Air Filters Using a High-Volume Flow Atomizer. *Aerosol Air Qual. Res.* **2019**, *19* (7), 1636–1644. https://doi.org/10.4209/aaqr.2019.04.0212.
(24) Merkl, P.; Long, S.; McInerney, G. M.; Sotiriou, G. A. Antiviral Activity of Silver, Copper Oxide and Zinc Oxide Nanoparticle Coatings against SARS-CoV-2. *Nanomaterials* **2021**, *11* (5), 1312. https://doi.org/10.3390/nano11051312.
(25) Byun, H. R.; Park, S. Y.; Hwang, E. T.; Sang, B. I.; Min, J.; Sung, D.; Choi, W. I.; Kim, S.; Lee, J. H. Antimicrobial Air Filter Coating with Plant Extracts Against Airborne Microbes. *Appl. Sci.* **2020**, *10* (24), 9120. https://doi.org/10.3390/app10249120.
(26) Lv, D.; Wang, R.; Tang, G.; Mou, Z.; Lei, J.; Han, J.; De Smedt, S.; Xiong, R.; Huang, C. Ecofriendly Electrospun Membranes Loaded with Visible-Light-Responding Nanoparticles for Multifunctional Usages: Highly Efficient Air Filtration, Dye Scavenging, and Bactericidal Activity. *ACS Appl. Mater. Interfaces* **2019**, *11* (13), 12880–12889. https://doi.org/10.1021/acsami.9b01508.
(27) Sun, Z.; Yue, Y.; He, W.; Jiang, F.; Lin, C.-H.; Pui, David. Y. H.; Liang, Y.; Wang, J. The Antibacterial Performance of Positively Charged and Chitosan Dipped Air Filter Media. *Build. Environ.* **2020**, *180*, 107020. https://doi.org/10.1016/j.buildenv.2020.107020.
(28) Rai, M.; Deshmukh, S. D.; Ingle, A. P.; Gupta, I. R.; Galdiero, M.; Galdiero, S. Metal Nanoparticles: The Protective Nanoshield against Virus Infection. *Crit. Rev. Microbiol.* **2016**, *42* (1), 46–56. https://doi.org/10.3109/1040841X.2013.879849.
(29) Rai, M.; Deshmukh, S. D.; Ingle, A. P.; Gupta, I. R.; Galdiero, M.; Galdiero, S. Metal Nanoparticles: The Protective Nanoshield against Virus Infection. *Crit. Rev. Microbiol.* **2016**, *42* (1), 46–56.
(30) Pal, S.; Tak, Y. K.; Song, J. M. Does the Antibacterial Activity of Silver Nanoparticles Depend on the Shape of the Nanoparticle? A Study of the Gram-Negative Bacterium Escherichia Coli. *Appl. Environ. Microbiol.* **2007**, *73* (6), 1712–1720.
(31) Bindhu, M. R.; Umadevi, M. Antibacterial Activities of Green Synthesized Gold Nanoparticles. *Mater. Lett.* **2014**, *120*, 122–125.
(32) MubarakAli, D.; Thajuddin, N.; Jeganathan, K.; Gunasekaran, M. Plant Extract Mediated Synthesis of Silver and Gold Nanoparticles and Its Antibacterial Activity against Clinically Isolated Pathogens. *Colloids Surf. B Biointerfaces* **2011**, *85* (2), 360–365.
(33) Chatterjee, A. K.; Chakraborty, R.; Basu, T. Mechanism of Antibacterial Activity of Copper Nanoparticles. *Nanotechnology* **2014**, *25* (13), 135101.
(34) Jung, W. K.; Koo, H. C.; Kim, K. W.; Shin, S.; Kim, S. H.; Park, Y. H. Antibacterial Activity and Mechanism of Action of the Silver Ion in Staphylococcus Aureus and Escherichia Coli. *Appl. Environ. Microbiol.* **2008**, *74* (7), 2171–2178.
(35) Crisan, C. M.; Mocan, T.; Manolea, M.; Lasca, L. I.; Tăbăran, F.-A.; Mocan, L. Review on Silver Nanoparticles as a Novel Class of Antibacterial Solutions. *Appl. Sci.* **2021**, *11* (3), 1120.
(36) Elechiguerra, J. L.; Burt, J. L.; Morones, J. R.; Camacho-Bragado, A.; Gao, X.; Lara, H. H.; Yacaman, M. J. Interaction of Silver Nanoparticles with HIV-1. *J. Nanobiotechnology* **2005**, *3* (1), 1–10.
(37) Fayaz, A. M.; Ao, Z.; Girilal, M.; Chen, L.; Xiao, X.; Kalaichelvan, P. T.; Yao, X. Inactivation of Microbial Infectiousness by Silver Nanoparticles-Coated Condom: A New Approach to Inhibit HIV- and HSV-Transmitted Infection. *Int. J. Nanomedicine* **2012**, *7*, 5007.
(38) Fatima, M.; Sadaf Zaidi, N.-S.; Amraiz, D.; Afzal, F. In Vitro Antiviral Activity of Cinnamomum Cassia and Its Nanoparticles against H7N3 Influenza a Virus. *J. Microbiol. Biotechnol.* **2016**, *26* (1), 151–159.
(39) Xiang, D.; Chen, Q.; Pang, L.; Zheng, C. Inhibitory Effects of Silver Nanoparticles on H1N1 Influenza A Virus in Vitro. *J. Virol. Methods* **2011**, *178* (1–2), 137–142.
(40) Almanza-Reyes, H.; Moreno, S.; Plascencia-López, I.; Alvarado-Vera, M.; Patrón-Romero, L.; Borrego, B.; Reyes-Escamilla, A.; Valencia-Manzo, D.; Brun, A.; Pestryakov, A.; Bogdanchikova, N.

Evaluation of Silver Nanoparticles for the Prevention of SARS-CoV-2 Infection in Health Workers: In Vitro and in Vivo. *PLOS ONE* **2021**, *16* (8), e0256401. https://doi.org/10.1371/journal.pone.0256401.

(41) *HeiQ Viroblock | Antiviral and Antibacterial Technology*. https://www.heiq.com/products/textile-technologies/heiq-viroblock-antiviral/?gclid=CjwKCAiA55mPBhBOEiwANmzoQs3WyDU0oxiSnKyQAWXAxfePDAO54f6K03S23b5NuKA_ezvMyhuUHhoC20IQAvD_BwE (accessed 2023-04-04).

(42) Balagna, C.; Perero, S.; Percivalle, E.; Nepita, E. V.; Ferraris, M. Virucidal Effect against Coronavirus SARS-CoV-2 of a Silver Nanocluster/Silica Composite Sputtered Coating. *Open Ceram.* **2020**, *1*, 100006–100006. https://doi.org/10.1016/j.oceram.2020.100006.

(43) Chen, Y.-N.; Hsueh, Y.-H.; Hsieh, C.-T.; Tzou, D.-Y.; Chang, P.-L. Antiviral Activity of Graphene–Silver Nanocomposites against Non-Enveloped and Enveloped Viruses. *Int. J. Environ. Res. Public. Health* **2016**, *13* (4), 430. https://doi.org/10.3390/ijerph13040430.

(44) Mori, Y.; Ono, T.; Miyahira, Y.; Nguyen, V. Q.; Matsui, T.; Ishihara, M. Antiviral Activity of Silver Nanoparticle/Chitosan Composites against H1N1 Influenza A Virus. *Nanoscale Res. Lett.* **2013**, *8* (1), 93. https://doi.org/10.1186/1556-276X-8-93.

(45) Jeremiah, S. S.; Miyakawa, K.; Morita, T.; Yamaoka, Y.; Ryo, A. Potent Antiviral Effect of Silver Nanoparticles on SARS-CoV-2. *Biochem. Biophys. Res. Commun.* **2020**, *533* (1), 195–200. https://doi.org/10.1016/j.bbrc.2020.09.018.

(46) Bekele, A. Z.; Gokulan, K.; Williams, K. M.; Khare, S. Dose and Size-Dependent Antiviral Effects of Silver Nanoparticles on Feline Calicivirus, a Human Norovirus Surrogate. *Foodborne Pathog. Dis.* **2016**, *13* (5), 239–244. https://doi.org/10.1089/fpd.2015.2054.

(47) Orlowski, P.; Tomaszewska, E.; Gniadek, M.; Baska, P.; Nowakowska, J.; Sokolowska, J.; Nowak, Z.; Donten, M.; Celichowski, G.; Grobelny, J.; Krzyzowska, M. Tannic Acid Modified Silver Nanoparticles Show Antiviral Activity in Herpes Simplex Virus Type 2 Infection. *PLoS ONE* **2014**, *9* (8), e104113. https://doi.org/10.1371/journal.pone.0104113.

(48) Chen, N.; Zheng, Y.; Yin, J.; Li, X.; Zheng, C. Inhibitory Effects of Silver Nanoparticles against Adenovirus Type 3 in Vitro. *J. Virol. Methods* **2013**, *193* (2), 470–477. https://doi.org/10.1016/j.jviromet.2013.07.020.

(49) Xiang, D.; Zheng, C.; Zheng, Y.; Li, X.; Yin, J.; O' Conner, M.; Marappan, M.; Miao, Y.; Xiang, B.; Duan, W.; Shigdar, S.; Zhao, X. Inhibition of A/Human/Hubei/3/2005 (H3N2) Influenza Virus Infection by Silver Nanoparticles in Vitro and in Vivo. *Int. J. Nanomedicine* **2013**, 4103. https://doi.org/10.2147/IJN.S53622.

(50) Sharma, V.; Kaushik, S.; Pandit, P.; Dhull, D.; Yadav, J. P.; Kaushik, S. Green Synthesis of Silver Nanoparticles from Medicinal Plants and Evaluation of Their Antiviral Potential against Chikungunya Virus. *Appl. Microbiol. Biotechnol.* **2019**, *103* (2), 881–891. https://doi.org/10.1007/s00253-018-9488-1.

(51) Murugan, K.; Dinesh, D.; Paulpandi, M.; Althbyani, A. D. M.; Subramaniam, J.; Madhiyazhagan, P.; Wang, L.; Suresh, U.; Kumar, P. M.; Mohan, J.; Rajaganesh, R.; Wei, H.; Kalimuthu, K.; Parajulee, M. N.; Mehlhorn, H.; Benelli, G. Nanoparticles in the Fight against Mosquito-Borne Diseases: Bioactivity of Bruguiera Cylindrica-Synthesized Nanoparticles against Dengue Virus DEN-2 (in Vitro) and Its Mosquito Vector Aedes Aegypti (Diptera: Culicidae). *Parasitol. Res.* **2015**, *114* (12), 4349–4361. https://doi.org/10.1007/s00436-015-4676-8.

(52) Hamouda, T.; Ibrahim, H. M.; Kafafy, H. H.; Mashaly, H. M.; Mohamed, N. H.; Aly, N. M. Preparation of Cellulose-Based Wipes Treated with Antimicrobial and Antiviral Silver Nanoparticles as Novel Effective High-Performance Coronavirus Fighter. *Int. J. Biol. Macromol.* **2021**, *181*, 990–1002. https://doi.org/10.1016/j.ijbiomac.2021.04.071.

(53) Lu, L.; Sun, R. W.-Y.; Chen, R.; Hui, C.-K.; Ho, C.-M.; Luk, J. M.; Lau, G. K. K.; Che, C.-M. Silver Nanoparticles Inhibit Hepatitis B Virus Replication. *Antivir. Ther.* **2008**, *13* (2), 253–262.

(54) Lv, X.; Wang, P.; Bai, R.; Cong, Y.; Suo, S.; Ren, X.; Chen, C. Inhibitory Effect of Silver Nanomaterials on Transmissible Virus-Induced Host Cell Infections. *Biomaterials* **2014**, *35* (13), 4195–4203. https://doi.org/10.1016/j.biomaterials.2014.01.054.

(55) Karagoz, S.; Kiremitler, N. B.; Sarp, G.; Pekdemir, S.; Salem, S.; Goksu, A. G.; Onses, M. S.; Sozdutmaz, I.; Sahmetlioglu, E.; Ozkara, E. S.; Ceylan, A.; Yilmaz, E. Antibacterial, Antiviral, and Self-Cleaning Mats with Sensing Capabilities Based on Electrospun Nanofibers Decorated with ZnO Nanorods and Ag Nanoparticles for Protective Clothing Applications. *ACS Appl. Mater. Interfaces* **2021**, *13* (4), 5678–5690. https://doi.org/10.1021/acsami.0c15606.

(56) Luceri, A.; Francese, R.; Lembo, D.; Ferraris, M.; Balagna, C. Silver Nanoparticles: Review of Antiviral Properties, Mechanism of Action and Applications. *Microorganisms* **2023**, *11* (3), 629. https://doi.org/10.3390/microorganisms11030629.
(57) Wei, L.; Lu, J.; Xu, H.; Patel, A.; Chen, Z.-S.; Chen, G. Silver Nanoparticles: Synthesis, Properties, and Therapeutic Applications. *Drug Discov. Today* **2015**, *20* (5), 595–601.
(58) Haggag, E. G.; Elshamy, A. M.; Rabeh, M. A.; Gabr, N. M.; Salem, M.; Youssif, K. A.; Samir, A.; Muhsinah, A. B.; Alsayari, A.; Abdelmohsen, U. R. Antiviral Potential of Green Synthesized Silver Nanoparticles of Lampranthus Coccineus and Malephora Lutea. *Int. J. Nanomedicine* **2019**, *14*, 6217.
(59) Galdiero, S.; Rai, M.; Gade, A.; Falanga, A.; Incoronato, N.; Russo, L.; Galdiero, M.; Gaikwad, S.; Ingle, A. Antiviral Activity of Mycosynthesized Silver Nanoparticles against Herpes Simplex Virus and Human Parainfluenza Virus Type 3. *Int. J. Nanomedicine* **2013**, 4303. https://doi.org/10.2147/IJN.S50070.
(60) Mori, Y.; Ono, T.; Miyahira, Y.; Nguyen, V. Q.; Matsui, T.; Ishihara, M. Antiviral Activity of Silver Nanoparticle/Chitosan Composites against H1N1 Influenza A Virus. *Nanoscale Res. Lett.* **2013**, *8* (1), 93. https://doi.org/10.1186/1556-276X-8-93.
(61) Acharya, D.; Mohanta, B.; Pandey, P.; Nasiri, F. Antibacterial Properties of Synthesized Ag and Ag@SiO2 Core–Shell Nanoparticles: A Comparative Study. *Can. J. Phys.* **2018**, *96* (8), 955–960. https://doi.org/10.1139/cjp-2017-0614.
(62) Tan, P.; Li, Y.-H.; Liu, X.-Q.; Jiang, Y.; Sun, L.-B. Core–Shell AgCl@SiO2 Nanoparticles: Ag(I)-Based Antibacterial Materials with Enhanced Stability. *ACS Sustain. Chem. Eng.* **2016**, *4* (6), 3268–3275. https://doi.org/10.1021/acssuschemeng.6b00309.
(63) Joe, Y. H.; Woo, K.; Hwang, J. Fabrication of an Anti-Viral Air Filter with SiO2–Ag Nanoparticles and Performance Evaluation in a Continuous Airflow Condition. *J. Hazard. Mater.* **2014**, *280*, 356–363. https://doi.org/10.1016/j.jhazmat.2014.08.013.
(64) Joe, Y. H.; Park, D. H.; Hwang, J. Evaluation of Ag Nanoparticle Coated Air Filter against Aerosolized Virus: Anti-Viral Efficiency with Dust Loading. *J. Hazard. Mater.* **2016**, *301*, 547–553. https://doi.org/10.1016/j.jhazmat.2015.09.017.
(65) Ferraris, M.; Balagna, C.; Perero, S. Method for the Application of an Antiviral Coating to a Substrate and Relative Coating. *WO2019082001Google Sch.* **2019**.
(66) Ferraris, M.; Chiaretta, D.; Fokine, M.; Miola, M.; Verné, E. Pellicole Antibatteriche Ottenute Da Sputtering e Procedimento per Conferire Proprietà Antibatteriche Ad Un Substrato. *TO2008A000098Google Sch.* **2008**.
(67) Ferraris, M.; Perero, S.; Miola, M.; Ferraris, S.; Vernè, E.; Morgiel, J. Silver Nanocluster–Silica Composite Coatings with Antibacterial Properties. *Mater. Chem. Phys. - MATER CHEM PHYS* **2010**, *120*, 123–126. https://doi.org/10.1016/j.matchemphys.2009.10.034.
(68) Ferraris, M.; Perero, S.; Miola, M.; Ferraris, S.; Gautier, G.; Maina, G.; Fucale, G.; Verne, E. Chemical, Mechanical, and Antibacterial Properties of Silver Nanocluster–Silica Composite Coatings Obtained by Sputtering. *Adv. Eng. Mater.* **2010**, *12* (7), B276–B282.
(69) Irfan, M.; Perero, S.; Miola, M.; Maina, G.; Ferri, A.; Ferraris, M.; Balagna, C. Antimicrobial Functionalization of Cotton Fabric with Silver Nanoclusters/Silica Composite Coating via RF Co-Sputtering Technique. *Cellulose* **2017**, *24* (5), 2331–2345.
(70) Balagna, C.; Perero, S.; Ferraris, S.; Miola, M.; Fucale, G.; Manfredotti, C.; Battiato, A.; Santella, D.; Vernè, E.; Vittone, E.; Ferraris, M. Antibacterial Coating on Polymer for Space Application. *Mater. Chem. Phys.* **2012**, *135* (2–3), 714–722. https://doi.org/10.1016/j.matchemphys.2012.05.049.
(71) Balagna, C.; Irfan, M.; Perero, S.; Miola, M.; Maina, G.; Crosera, M.; Santella, D.; Simone, A.; Ferraris, M. Antibacterial Nanostructured Composite Coating on High Performance Vectran™ Fabric for Aerospace Structures. *Surf. Coat. Technol.* **2019**, *373*, 47–55.
(72) Muzio, G.; Perero, S.; Miola, M.; Oraldi, M.; Ferraris, S.; Vernè, E.; Festa, F.; Canuto, R. A.; Festa, V.; Ferraris, M. Biocompatibility versus Peritoneal Mesothelial Cells of Polypropylene Prostheses for Hernia Repair, Coated with a Thin Silica/Silver Layer. *J. Biomed. Mater. Res. B Appl. Biomater.* **2017**, *105* (6), 1586–1593. https://doi.org/10.1002/jbm.b.33697.
(73) Baino, F.; Ferraris, S.; Miola, M.; Perero, S.; Verné, E.; Coggiola, A.; Dolcino, D.; Ferraris, M. Novel Antibacterial Ocular Prostheses: Proof of Concept and Physico-Chemical Characterization. *Mater. Sci. Eng. C* **2016**, *60*, 467–474.

(74) Balagna, C.; Irfan, M.; Perero, S.; Miola, M.; Maina, G.; Santella, D.; Simone, A. Characterization of Antibacterial Silver Nanocluster/Silica Composite Coating on High Performance Kevlar® Textile. *Surf. Coat. Technol.* **2017**, *321*, 438–447.
(75) Balagna, C.; Perero, S.; Bosco, F.; Mollea, C.; Irfan, M.; Ferraris, M. Antipathogen Nanostructured Coating for Air Filters. *Appl. Surf. Sci.* **2020**, *508*, 145283. https://doi.org/10.1016/j.apsusc.2020.145283.
(76) Balagna, C.; Francese, R.; Perero, S.; Lembo, D.; Ferraris, M. Nanostructured Composite Coating Endowed with Antiviral Activity against Human Respiratory Viruses Deposited on Fibre-Based Air Filters. *Surf. Coat. Technol.* **2021**, *409*, 126873. https://doi.org/10.1016/j.surfcoat.2021.126873.
(77) NCCLS M2-A9, Performance Standards for Antimicrobial Disk Susceptibility Tests, Approved Standard, 9th Edn, NCCLS, Villanova, PA, USA 2003
(78) NCCLS M7-A6, MethodNCCLS M7-A6, Methods for Dilution Antimicrobial Susceptibility Tests for Bacteria that grow Aerobically, Approved standard 6th ed. NCCLS, Villanova, PA, USA 2003s for Dilution Antimicrobial Susceptibility Tests for Bacteria that grow Aerobically, Approved standard 6th ed. NCCLS, Villanova, PA, USA 2003
(79) Liu, D. X.; Liang, J. Q.; Fung, T. S. Human Coronavirus-229E, -OC43, -NL63, and -HKU1 (Coronaviridae). *Encycl. Virol.* **2021**, 428–440. https://doi.org/10.1016/B978-0-12-809633-8.21501-X.
(80) Fung, T. S.; Liu, D. X. Similarities and Dissimilarities of COVID-19 and Other Coronavirus Diseases. *Annu. Rev. Microbiol.* **2021**, *75*, 19–47. https://doi.org/10.1146/annurev-micro-110520-023212.
(81) Raza, M. A.; Kanwal, Z.; Rauf, A.; Sabri, A. N.; Riaz, S.; Naseem, S. Size- and Shape-Dependent Antibacterial Studies of Silver Nanoparticles Synthesized by Wet Chemical Routes. *Nanomaterials* **2016**, *6* (4), 74. https://doi.org/10.3390/nano6040074.
(82) Ferdous, Z.; Nemmar, A. Health Impact of Silver Nanoparticles: A Review of the Biodistribution and Toxicity Following Various Routes of Exposure. *Int. J. Mol. Sci.* **2020**, *21* (7), 2375. https://doi.org/10.3390/ijms21072375.

Figure captions

Fig.1: FESEM of the glass-fibre filters (a) Glass and (b) Glass-Ag5; polymeric filter (c) Pol and (d) Pol-Ag3

Fig.2: Test on the release of silver ions into water at room temperature from a silver nanocluster/silica composite coating on glass-fibre and polymeric air filters.

Fig.3: Inhibition halo test results against *S. epidermidis* and *E. coli*: (a) uncoated and coated glass fibre filters; (b) uncoated and coated polymeric filters.

Fig.4: CFU count against *S. epidermis* of both the uncoated and coated glass-fibre and polymeric air filters: (a) broth solution used to evaluate bacteria proliferation; (b) vortex solution used to evaluate the adhesion of bacteria onto the sample surfaces.

Fig. 5: Contamination test with *S. epidermidis* through bioaerosol generator on (a) uncoated and coated glass-fibre filter and (b) uncoated and coated polymeric membrane

Fig. 6: Virucidal assay in an aqueous medium. Comparison of the coated and the uncoated samples. " Untreated" refers to the viral particles incubated under the same temperature and time conditions, but without testing any samples. The viral titre is reported on the Y-axis and expressed as focus forming units per ml (FFU/ml). The type of sample is reported on the X-axis. ***pANOVA<0.001;*pANOVA<0.05; ns: not significant.

Fig. 7: Virucidal assay conducted by means of a drying method (a) and Ion release antiviral test (b). The coated and the uncoated samples are compared. "Untreated" refers to the viral particles incubated under the same temperature and time experimental conditions, but without testing any samples. The viral titre is reported on the Y-axis and expressed as focus forming units per ml (FFU/ml). The sample type is reported on the X-axis. ****pANOVA<0.0001 ***pANOVA<0.001; **pANOVA<0.01; ns: not significant.

Table 1: Atomic percentage of the silicon and silver of the uncoated and coated glass-fibre and polymeric air filters (EDS analysis).

	atomic %				
Element	**Glass**	**Glass-Ag3**	**Glass-Ag5**	**Pol**	**Pol-Ag3**
Si	10.06 ± 0.22	12.14 ± 0.65	12.04 ±0.72	/	0.98 ± 0.03
Ag	/	0.94 ± 0.01	1.62 ± 0.03	/	0.78 ± 0.03

Table 2: Numerical results of the virucidal assay in an aqueous medium

Sample	HCoV-OC43 titer	Logarithm of inactivation (R)
Untreated virus	$(3.5 \pm 0.4) \times 10^6$	
Glass	$(4.6 \pm 1.1) \times 10^6$	
Glass-Ag3	$(7.6 \pm 1.5) \times 10^5$	0.79
Glass-Ag5	$(6.2 \pm 0.9) \times 10^5$	0.87
Pol	$(3.7 \pm 0.4) \times 10^6$	
Pol-Ag3	$(3.0 \pm 0.2) \times 10^5$	1.1

Table 3: Numerical results of the virucidal assay, conducted by means of a drying method, and of the ion release antiviral test.

Sample	HCoV-OC43 titer			
	Drying method	Logarithm of inactivation (R)	Ion release	Logarithm of inactivation (R)
Untreated virus/CTRL(DMEM)	$(1.9 \pm 0.4) \times 10^5$		$(6.1 \pm 0.5) \times 10^4$	
Glass	$(3.2 \pm 0.7) \times 10^4$		$(7.2 \pm 1.0) \times 10^4$	
Glass-Ag5	$(1.7 \pm 0.5) \times 10^4$	0.27	$(1.5 \pm 0.7) \times 10^4$	0.67
Pol	$(1.9 \pm 0.2) \times 10^5$		$(6.2 \pm 0.6) \times 10^4$	
Pol-Ag3	$(8.1 \pm 2.5) \times 10^4$	1.38	$(2.1 \pm 0.7) \times 10^4$	0.46

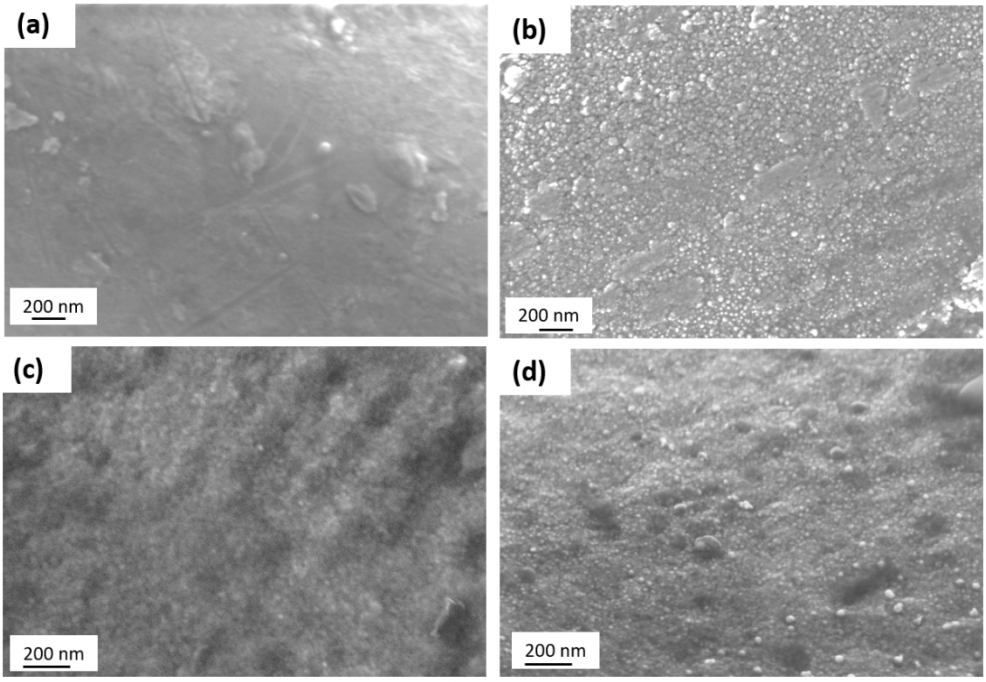


Fig.1: FESEM of the glass-fibre filters (a) Glass and (b) Glass-Ag5; polymeric filter (c) Pol and (d) Pol-Ag3

105x73mm (300 x 300 DPI)

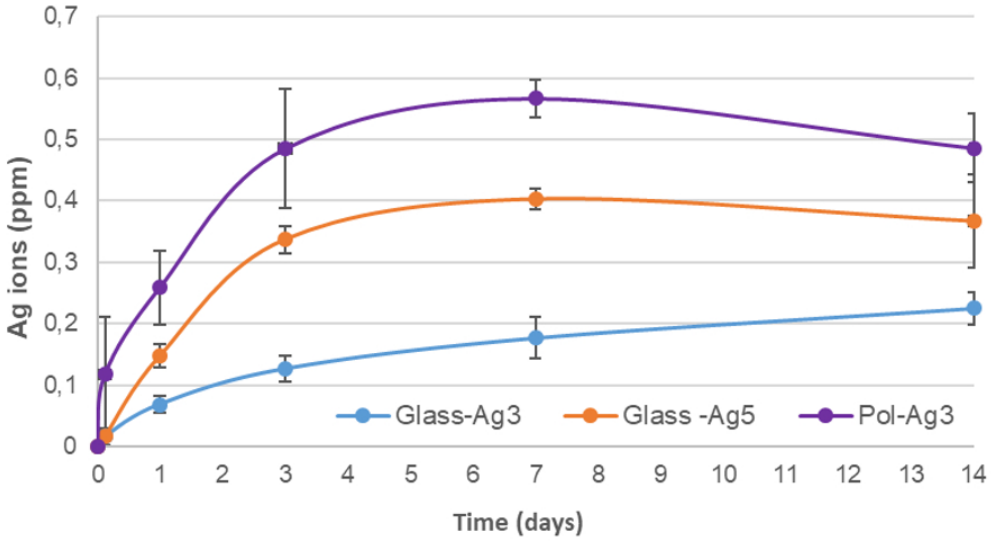


Fig.2: Test on the release of silver ions into water at room temperature from a silver nanocluster/silica composite coating on glass-fibre and polymeric air filters.

75x40mm (300 x 300 DPI)

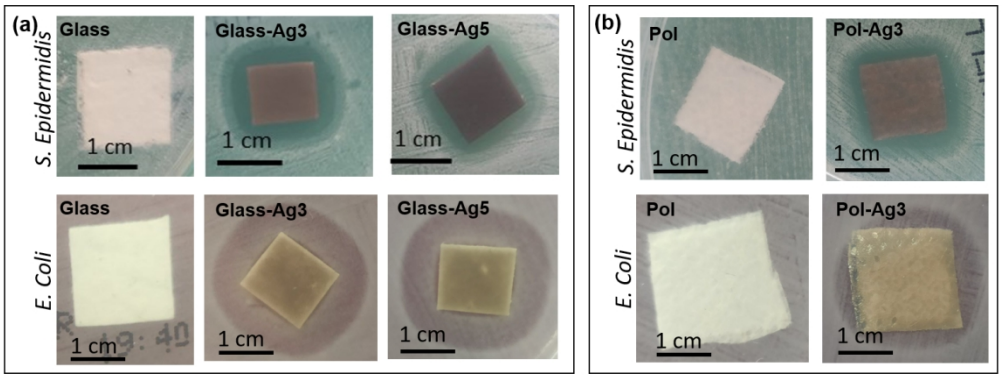


Fig.3: Inhibition halo test results against S. epidermidis and E. coli: (a) uncoated and coated glass fibre filters; (b) uncoated and coated polymeric filters.

131x50mm (300 x 300 DPI)

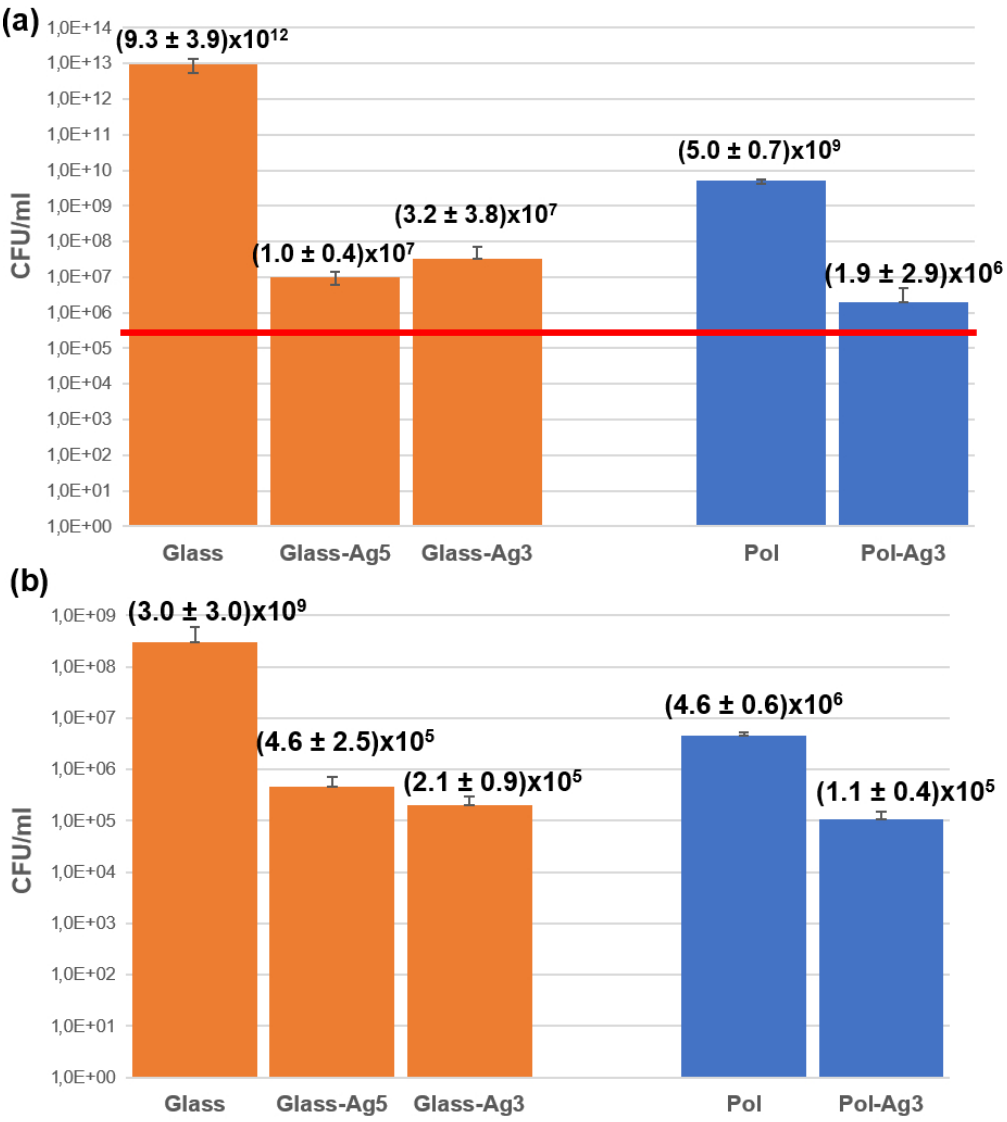


Fig.4: CFU count against S. epidermis of both the uncoated and coated glass-fibre and polymeric air filters: (a) broth solution used to evaluate bacteria proliferation; (b) vortex solution used to evaluate the adhesion of bacteria onto the sample surfaces.

77x91mm (300 x 300 DPI)

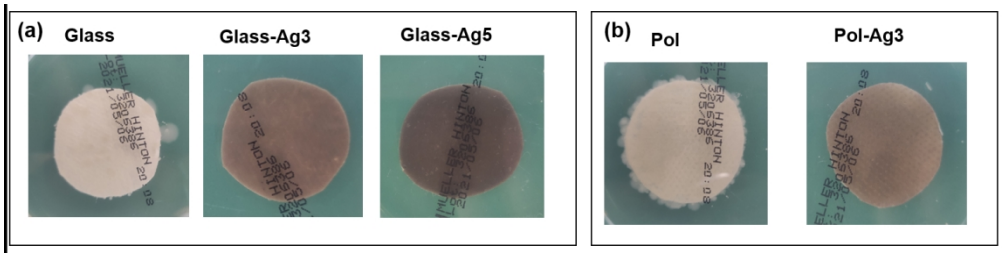


Fig. 5: Contamination test with S. epidermidis through bioaerosol generator on (a) uncoated and coated glass-fibre filter and (b) uncoated and coated polymeric membrane

132x32mm (300 x 300 DPI)

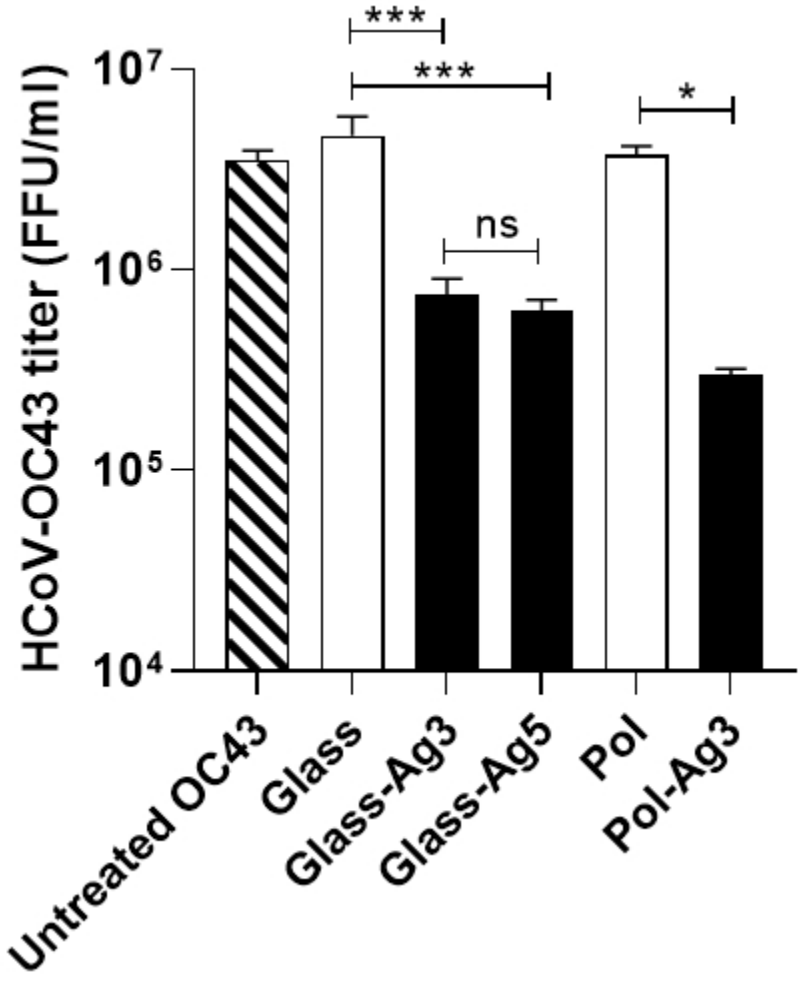


Fig. 6: Virucidal assay in an aqueous medium. Comparison of the coated and the uncoated samples. " Untreated" refers to the viral particles incubated under the same temperature and time conditions, but without testing any samples. The viral titre is reported on the Y-axis and expressed as focus forming units per ml (FFU/ml). The type of sample is reported on the X-axis. ***pANOVA<0.001;*pANOVA<0.05; ns: not significant.

37x43mm (300 x 300 DPI)

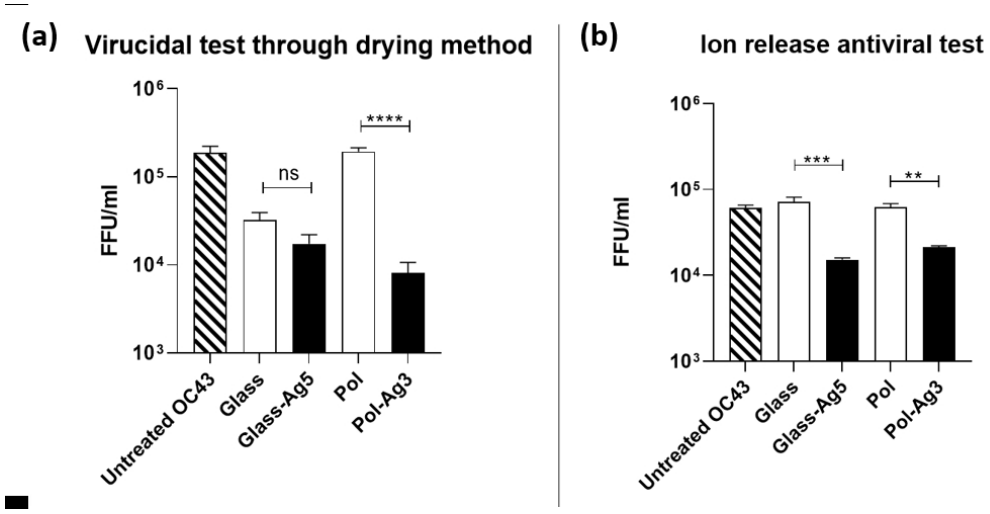
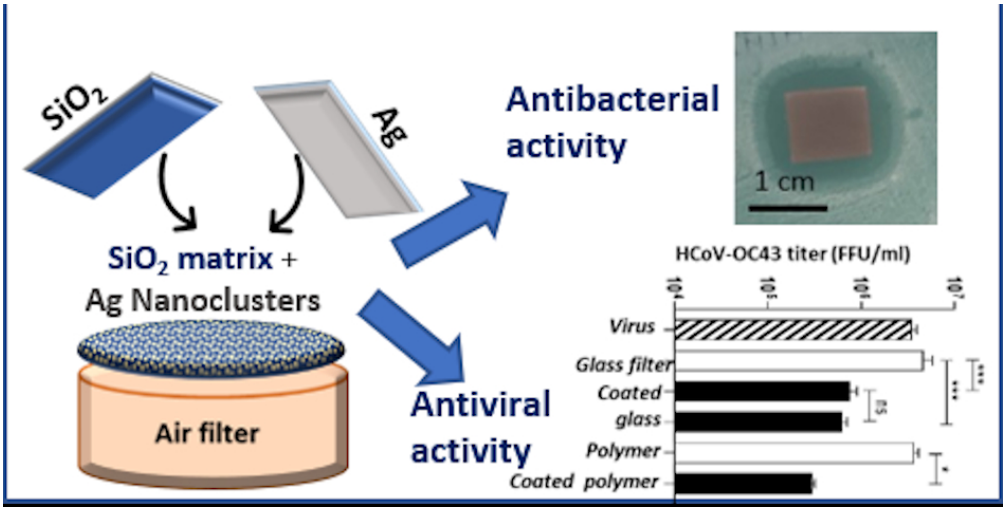


Fig. 7: Virucidal assay conducted by means of a drying method (a) and Ion release antiviral test (b). The coated and the uncoated samples are compared. "Untreated" refers to the viral particles incubated under the same temperature and time experimental conditions, but without testing any samples. The viral titre is reported on the Y-axis and expressed as focus forming units per ml (FFU/ml). The sample type is reported on the X-axis. ****pANOVA<0.0001 ***pANOVA<0.001; **pANOVA<0.01; ns: not significant.

83x42mm (300 x 300 DPI)



80x40mm (300 x 300 DPI)